Apoptosis (2012) 17:449–462
DOI 10.1007/s10495-012-0699-0

ORIGINAL PAPER

Mechanisms to prevent caspase activation in rotenone-induced dopaminergic neurodegeneration: role of ATP depletion and procaspase-9 degradation

HeeWon Kang · Baek-Soo Han · Su-Jeong Kim · Young J. Oh

Published online: 1 February 2012

Abstract The evidence implicating a mode of cell death that either favors or argues against caspase-dependent apoptosis is available in studies that used experimental models of Parkinson's disease. We sought to investigate the mechanisms by which release of cytochrome *c* is not linked to caspase activation during rotenone-induced dopaminergic (DA) neurodegeneration. Unlike caspase activation in 6-hydroxydopamine-treated cells, both MN9D DA neuronal cells and primary cultures of mesencephalic neurons showed no obvious signs of caspase activation upon exposure to rotenone. We found that intracellular levels of ATP significantly decreased at the early phase of neurodegeneration ($<\sim$24 h) and therefore external addition of ATP to the lysates obtained at this stage reconstituted caspase-3 activity. At a later phase of cell death ($>\sim$24 h), both decreased levels of ATP and procaspase-9 contributed to the lack of caspase-3 activation. Under this condition, calpain and the proteasome system were responsible for the degradation of procaspase-9. Consequently, external addition of ATP and procaspase-9 to the lysates harvested at the later phase was required for activation of caspase-3. Similarly, caspase-3 activity was also reconstituted in the lysates harvested from cells co-treated with inhibitors of these proteases and incubated in the presence of external ATP. Taken together, our findings provided a sequential mechanism underlying how DA neurons may undergo caspase-independent cell death, even in the presence of cytoplasmic cytochrome *c* following inhibition of mitochondrial complex I.

Keywords Neurodegeneration · Mitochondrial complex I inhibitor · Calpain · Proteasome

Introduction

Parkinson's disease (PD) is a common neurodegenerative disorder characterized by pathological hallmarks such as the progressive loss of dopaminergic (DA) neurons in the substantia nigra pars compacta and formation of Lewy bodies [1]. Most PD cases are sporadic and its etiology is incompletely understood; however, an increasing body of evidence suggests that oxidative stress, mitochondrial dysfunction, inflammation and abnormal protein aggregation may be involved in the pathogenesis of PD [1]. Interestingly, many of the familial PD genes have been also linked to management of reactive oxygen species (ROS) generation, mitochondrial function, and protein folding, sharing common pathways underlying the pathogenesis of sporadic forms of PD [2]. In any cases, several cell death modes, including apoptosis, necrosis and autophagy, have been demonstrated during DA neurodegeneration [3].

Neurotoxin-based experimental models have been widely used to study biochemical changes reminiscent of those occurring in patients with PD [1]. Among the neurotoxins shown to cause neurodegeneration, 6-hydroxydopamine (6-OHDA) was the first used to establish an animal model of PD associated with DA neuronal death in

HeeWon Kang, Baek-Soo Han, and Su-Jeong Kim contributed equally to this article.

H. Kang · S.-J. Kim · Y. J. Oh (✉)
Department of Biology, Yonsei University College of Life Science and Biotechnology, Seoul 120-749, Korea
e-mail: yjoh@yonsei.ac.kr

B.-S. Han
Brain Research Center, Korea Research Institute of Bioscience and Biotechnology, Daejeon 305-806, Korea

the substantia nigra pars compacta [4]. Once accumulated inside DA neurons, 6-OHDA is involved in the generation of ROS including autooxidation, leading to cell death typical of apoptosis. Systemic administration of the mitochondrial complex I toxin, 1-methyl-4-phenyl-1,2,3,6-tetrahydropyridine (MPTP), into non-human primates and mice has been also used to produce animal models of PD [5]. Once in the brain, MPTP is oxidatively metabolized into its active toxic molecule, 1-methyl-4-phenylpyridinium (MPP^+) via monoamine oxidase B present in glial cells. Betarbet et al. [6] demonstrated that low-dose intravenous administration of rotenone to rats produces selective degeneration of nigrostriatal DA neurons, PD-like locomotor behavior, and occurrence of cytoplasmic inclusions. Recently, progression of disease pathology has been also reproduced in mice after low dose of chronic and intragastric administration of rotenone [7]. Similarly, it has been demonstrated that sublethal, chronic exposure to rotenone induces widespread loss of DA neurons and severe locomotor deficits in Drosophila, mimicking several key aspects of PD [8]. Subsequently, rotenone has been proposed to produce apoptosis potentially via oxidative damage, endoplasmic reticulum stress and abnormal protein aggregation in cellular models of PD [9, 10].

It has been widely accepted that ROS per se and ROS-mediated apoptotic signaling underlie the major neurotoxic mechanism following 6-OHDA treatment and this has been demonstrated both in a wide variety of cells and in rat brain models [1]. In contrast, the evidence implicating a mode of cell death that either favors or argues against caspase-dependent apoptosis is available in studies that used experimental models generated by the mitochondrial complex I toxins. For example, several studies suggest that apoptosis may reflect the primary mechanisms closely associated with mitochondrial complex I toxin-induced DA neuronal death [11–13]. Several other reports still including ones from our laboratory conflict with regard to mitochondrial complex I toxin-induced cell death and indicate non-apoptotic DA neuronal death [14–18]. Although the exact nature of this controversy is not clearly understood, the interpretation of whether the mitochondrial complex I toxins elicit apoptosis should be regarded with caution. Therefore, the specific aim of the present study was to examine the molecular mechanism underlying mitochondrial complex I inhibitor-induced DA neuronal cell death using both the MN9D DA neuronal cell line and primary cultures of DA neurons. Here, we present evidence indicating that sequential depletion of intracellular ATP, and protease-mediated degradation of procaspase-9, may be responsible for the lack of caspase activation following cytosolic release of cytochrome *c* in mitochondrial complex I inhibitor-induced MN9D DA neuronal death.

Materials and methods

Cell cultures and drug treatments

MN9D cells [14] were seeded on 25 μg/ml poly-D-lysine-coated culture dishes or plates (Corning Glass Works, Corning, NY, USA), maintained in DMEM supplemented with 10% FBS (Invitrogen, San Diego, CA, USA) in an incubator with an atmosphere of 10% CO_2 at 37°C, and switched to serum-free N2 medium [14] containing various experimental reagents. Primary cultures of DA neurons were prepared from the ventral mesencephalon of 14 d gestation Sprague Dawley rat embryos and processed for drug treatment as previously described [17]. Reagents used included rotenone, MPP^+, 6-OHDA (all from Sigma, St. Louis, MO, USA), BAPTA-AM (Molecular Probes, Eugene, OR, USA), calpeptin, clasto-lactacystin-β-lactone (lactacystin), and MG132 (all from Calbiochem, La Jolla, CA, USA).

Electron microscopy and propidium iodide staining

MN9D cells plated onto the poly-D-lysine-coated 35 mm culture plate (SPL Life Sciences Inc., Korea) were treated with 10 nM rotenone for the indicated time periods. Cells were then washed with DMEM and fixed with a buffer containing 2% paraformaldehyde and 0.5% glutaraldehyde in 0.1 M cacodylate buffer, post-fixed with 1% osmium tetroxide and en bloc stained with 0.2% uranyl acetate solution. Subsequently, cells were dehydrated with an ascending ethanol series and embedded with an Epon mixture. Thin sections of 80 nm were obtained using a Reichert-Jung Ultracut E microtome (Leica, Wetzlar, Germany). Sections were mounted on a 200-mesh grid and stained with uranyl acetate followed by lead citrate. Electron microscopic photomicrographs were taken with a Hitachi H-7500 (Hitachi, Japan) TEM with 80 kV acceleration voltage. For propidium iodide (PI) staining, cells were gently washed with warm DMEM and incubated with 3 μl of 2 mg/ml PI (Sigma) at room temperature for 3 min in the dark, and rinsed with warm PBS. Stained cells were examined under an Axio Observer A1 microscope equipped with epifluorescence and a digital image analyzer (Carl Zeiss, Zena, Germany).

Immunoblot analysis

Following drug treatments, MN9D cells washed with ice-cold PBS were subjected to lysis on ice in a buffer containing RIPA buffer (50 mM Tris–HCl, pH 7.4, 1 mM EGTA, 1% NP-40, 0.25% sodium deoxycholate, 150 mM NaCl, and 0.1% SDS) with the Complete mini-EDTA-free protease inhibitor cocktail tablets (Roche Applied Science,

Mannheim, Germany). Cells were homogenized in a Douncer on ice, followed by centrifugation at 13,000×*g* for 10 min at 4°C. For detecting cytochrome *c* release, cellular fractionation was performed as previously described [17] with minor modifications. Protein contents were measured using a Bio-Rad protein assay kit (Bio-Rad Laboratories, Hercules, CA, USA). Fifty to seventy-five micrograms of protein were separated on a 7–12.5% SDS-PAGE, blotted onto pre-wetted PVDF-nitrocellulose filters, and processed for immunoblot analysis. Primary antibodies used were a rabbit polyclonal anti-procaspase-9, anti-cleaved caspase-3, anti-cleaved caspase-9 (1:1,000; all from Cell Signaling, Beverly, MA, USA), a rabbit polyclonal anti-calpain cleaved fodrin (a generous gift from Dr. Saido at RIKEN, Japan), a mouse monoclonal anti-cytochrome *c* (1:3,000; PharMingen, San Diego, CA, USA), anti-Apaf-1 (1:1,000; Chemicon International, Temecula, CA, USA), and a mouse monoclonal anti-ubiquitin (P4D1) (1:1,000; Santa Cruz Biotechnology, Santa Cruz, CA, USA). A mouse monoclonal anti-glyceraldehyde-3-phosphate dehydrogenase (GAPDH; 1:3,000; Chemicon International) was used as a loading control. Both a mouse monoclonal anti-cytochrome oxidase subunit IV (COX-IV, 1:1,000; Molecular Probes) and a rabbit polyclonal anti-superoxide dismutase 1 (SOD-1, 1:1,000; Santa Cruz Biotechnology) were used as fraction markers for the mitochondria and the cytosol, respectively. Specific bands were detected by enhanced chemiluminescence (ECL; Amersham Pharmacia Biotech, Piscataway, NJ, USA). The intensities of bands were analyzed using Image J. Values were normalized by the corresponding levels of GAPDH or SOD-1 (for Fig. 4b) and expressed as the average fold difference in band intensity of the corresponding proteins over the controls (1.00).

Quantification of tyrosine hydroxylase (TH)-immunoreactive neurons and DA uptake assay

To determine the number of surviving DA neurons following drug treatment, primary cultures of DA neurons were subjected to immunocytochemical localization of TH, the rate-limiting enzyme of dopamine biosynthesis, and cell counting as previously described [17]. Briefly, manual counts by an individual blind to the treatment conditions were carried out of all of the TH-positive cells having neurites twice the length of the soma. For measuring the rate of DA uptake, cells were incubated with 25 nM [^{3}H]DA (45 Ci/mmol; Amersham Biosciences, Buckinghamshire, UK) for 15 min in Krebs–Ringer solution after treatment of DA neurons with the indicated concentrations of rotenone. The resulting radioactivity was quantified by a liquid scintillation counter (Beckman, Fullerton, CA, USA), as previously described [17].

ATP measurement

Luminometric measurement of intracellular ATP levels was determined using ATP Determination Kit and carried out according to the protocol provided by the manufacturer (Molecular Probes). Briefly, after drug treatments, MN9D cells were dissociated with 0.25% trypsin, lysed in a buffer containing 10 mM KH_2PO_4, 4 mM $MgSO_4$, and then boiled at 95°C for 5 min. Cellular lysates were incubated on ice for 5 min, and transferred into luminometer vials. Ten microliters of cellular lysates were mixed well with 100 µl of reaction solution provided by manufacturer. The luminometric values were quantified by a TD-20/20 luminometer (Turner Designs Instrument, Sunnyvale, CA, USA). Values from each treatment were expressed as a percentage over the untreated control at each time point (100%).

Immunocytochemistry for activated caspase-3 and fluorescent staining of intracellular free calcium

After drug treatments, MN9D cells were fixed with 4% paraformaldehyde for 20 min at RT, and blocked for 1 h in PBS containing 5% normal goat serum and 0.2% Triton X-100. Cells were then incubated with the primary antibody in PBS containing 1% normal goat serum and 0.2% Triton X-100 at 4°C overnight. A rabbit polyclonal antibody that recognizes the cleaved forms of activated caspase-3 was used as the primary antibody (1:200; Cell signaling). After washes with PBS, cells were incubated at RT for 1 h with Alexa Fluor 488® goat anti-mouse IgG (1:200; Molecular Probes). To visualize the nuclei, MN9D cells were incubated with 1 µg/ml Hoest33258 (Molecular Probes) in PBS for 5 min. For immunocytochemical localization of the cleaved forms of activated caspase-3 among TH-positive neurons, primary cultures of DA neurons were subjected to double immunofluorescent staining using antibodies that recognize the cleaved form of caspase-3 (1:200; Cell signaling) and TH (1:7,500; Pel-Freez, Rogers, AR, USA) followed by incubation with Alexa Fluor 488® goat anti-mouse IgG and Alexa Fluor 594® goat anti-rabbit IgG. Cells were examined under an AxioImager D1 microscope equipped with an epifluorescence unit and Axiocam Digital Camera (Carl Zeiss). To label the cytosolic free calcium, toxin-treated MN9D cells were loaded with 3 µM Flou-3/AM dye (Molecular Probe) in N2 medium for 30 min at 37°C in an incubator with an atmosphere of 10% CO_2, and washed two times with N2 media according to the protocol provided by the manufacturer. Cells were then examined under an Axiovert 100 microscope equipped with an epifluorescence unit and Axiocam Digital Camera (Carl Zeiss).

In vitro and cell-based calpain cleavage assays

Metabolically labeled procaspase-9 was produced using an in vitro transcription and translation kit according to the instruction of the manufacturer (Promega, Madison, WI, USA) using the plasmid containing HA-tagged human procaspase-9 in pcDNA 3. The labeled products were subjected to an in vitro calpain cleavage assay. Briefly, 5 μl of [^{35}S]-labeled procaspase-9 was incubated with 0.134 unit of porcine μ- or 0.343 unit of m-calpain (all from Calbiochem) in the presence or the absence of 1 mM $CaCl_2$ and 5 μM calpeptin (Calbiochem; a calpain inhibitor). Basically, the reaction mixture was made up to a final volume of 30 μl with calpain reaction buffer (25 mM Tris, 10 mM KCl, 10 mM $CaCl_2$, and 0.1% Triton-X 100) and incubated at 30°C for the indicated time periods. Six microliters of 5× SDS-loading buffer was added and the reaction mixture was subjected to 8% SDS-PAGE. For autoradiography, gels were dried on 3 M paper, exposed to X-ray film overnight, and developed. For cell-based calpain cleavage assays, MN9D cells were washed with ice-cold PBS and lysed in a buffer containing 50 mM Tris, pH 7.0, 2 mM EDTA, and 1% Triton X-100 without any protease inhibitors. Cells were homogenized in a Douncer on ice and centrifuged at 13,000×g for 10 min at 4°C. Fifty micrograms of protein were incubated for 2 h at 37°C with 1 mM $CaCl_2$ and 2 μl of μ-calpain or m-calpain in the presence or absence of various protease inhibitors including 50 μM calpeptin, 2.5 μM MG132 or 2.5 μM lactacystin. Reaction mixtures were subjected to immunoblot analysis for procaspase-9.

In vitro and cell-based ubiquitination assays

Metabolically labeled procaspase-9 was incubated and assayed for polyubiquitination using the Ubiquitin Protein Conjugation Kit according to the manufacturer's instruction (Calbiochem). Briefly, 5 μl of [^{35}S]-labeled procaspase-9 was incubated at 37°C for 1 h in a total volume of 30 μl reaction buffer with or without 25 μl ubiquitination cocktail containing E1, E2, and E3 components, and 3 μl ubiquitin aldehyde. Six microliters of 5× SDS-loading buffer was added and the reaction mixture was subjected to 8% SDS-PAGE. For autoradiography, gels were dried on 3 M paper, exposed to X-ray film overnight, and developed. For cell-based ubiquitination assays, MN9D cells were first transiently transfected with pEF/HA-ubiquitin, and then treated with the indicated toxins in the presence of a proteasome inhibitor, lactacystin. After several washes with PBS, cells were lysed on ice for 30 min in a RIPA buffer containing a protease inhibitor cocktail and without SDS. After centrifugation at 13,000×g for 10 min at 4°C, 3 mg cell lysates in 1 ml was precleared with 40 μl of 50% Protein A agarose, which was washed five times with RIPA buffer without SDS (Upstate, Temecula, CA, USA). After centrifugation, the supernatant was incubated with 3 μg of a mouse monoclonal anti-caspase-9 (Chemicon) at 4°C overnight, incubated with 40 μl of 50% Protein A agarose for 2 h, and washed three times with RIPA buffer without SDS. The pellet was dissolved with 30 μl of 1× sample buffer and half of each sample was separated on 8% SDS-PAGE. Blots were probed with a mouse monoclonal anti-ubiquitin (P4D1; 1:1,000; Santa Cruz Biotechnology) and a rabbit polyclonal anti-procaspase-9 (1:1,000, Cell Signaling), respectively.

In vitro reconstitution assay of caspase-3

After treatment with 10 nM rotenone in the presence or the absence of the indicated protease inhibitors, cell lysates were prepared as described and an in vitro reconstitution assay of caspase activity was performed as previously described [17] with some modifications. Briefly, cellular lysates (50 μg) were incubated for 2 h at 30°C in a reaction buffer containing 20 mM HEPES-KOH, pH 7.5, 10 mM KCl, 1.5 mM $MgCl_2$, 1 mM EDTA, 1 mM EGTA, and 1 mM dithiothreitol containing 1 mM ATP alone or in combination with 31.25 ng procaspase-9. The reaction mixtures were subjected to an immunoblot analysis for the cleaved caspase-3.

Statistical analysis

All the data represent the mean ± SEM from at least three independent experiments. Statistical analysis was performed by one-way ANOVA followed by Tukey's multiple comparison test.

Results

Lack of caspase activation in rotenone-treated MN9D dopaminergic neuronal cells

Rotenone is a well-known inhibitor of mitochondrial complex I and have been utilized to establish experimental models of PD [1]. To determine a dose- and time-responsiveness, MN9D cells were treated with a wide concentration range of rotenone (1–100 nM) for up to 48 h. At 10–100 nM rotenone, a great majority of MN9D cells were positive for PI staining, indicating that cells were dead or damaged. As shown in Fig. 1a, cells were not obviously stained for PI following 10 nM rotenone treatment for 24 h, indicating that at this time point a great majority of cells still have an intact membrane. In contrast, approximately 20% of cells were stained positive for PI at 36 h and

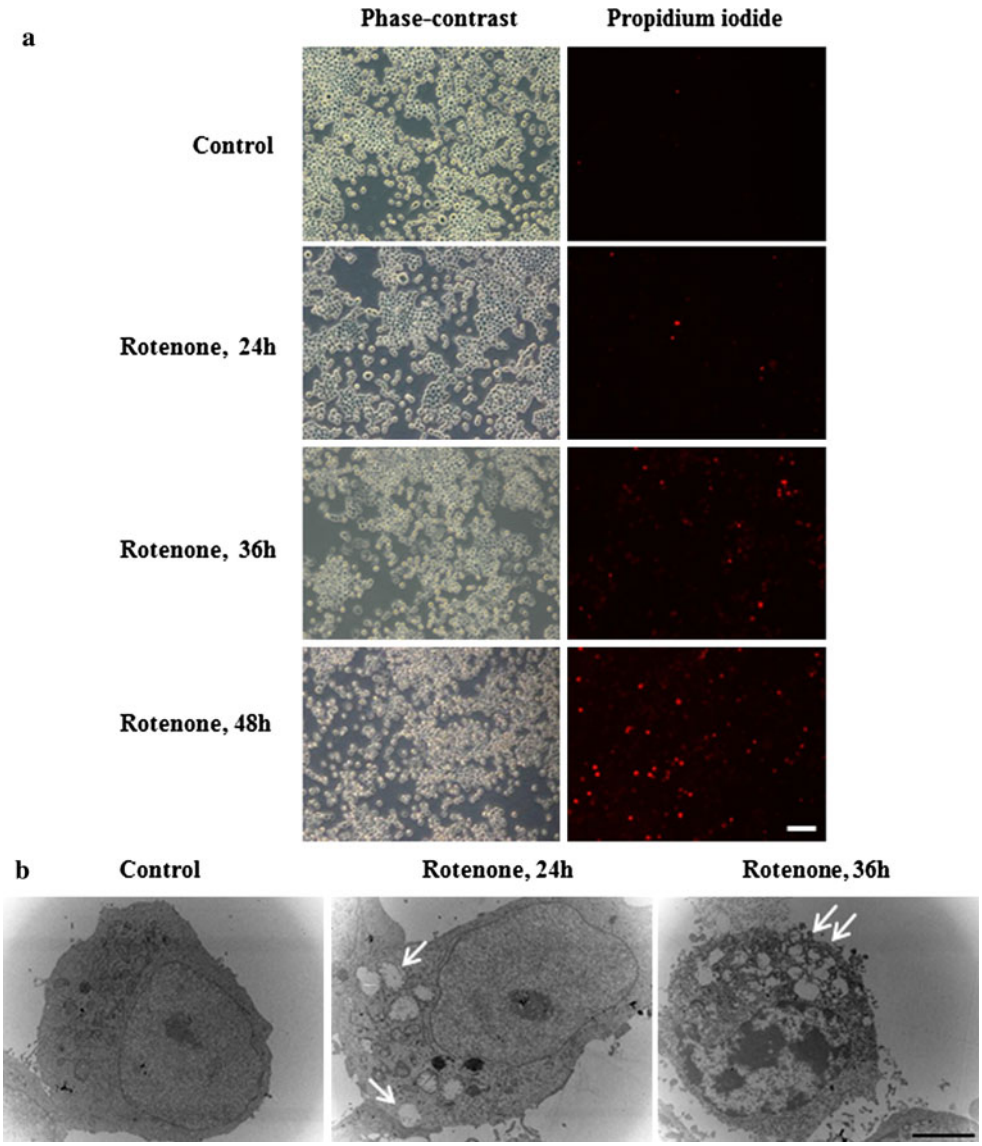

Fig. 1 Morphological characterization of rotenone-induced DA neurodegeneration. MN9D cells treated with 10 nM rotenone were subjected to PI analyses and electron microscopy. **a** Cells were incubated with PI to stain nuclei of the cells with the disrupted cytoplasmic membrane. Photomicrographs demonstrate a time-dependent increase of PI-positive cells. *Scale bar* 100 μm. **b** Twenty-four or thirty-six hours after drug treatment, transmission electron micrographs were taken. *Single arrow* and *double arrows* indicate the swollen mitochondria and disrupted membrane, respectively. *Scale bar* 5 μm

number of PI-positive cells increased thereafter. As determined by morphological criteria, rotenone caused quite distinct changes in morphology, with the apparent appearance of vacuole-like structures within the cytoplasm and no obvious signs of shrunken nuclei under a phase-contrast microscope. This was in contrast to the shrunken nuclei typically observed in MN9D cells treated with 100 μM 6-OHDA [14, 17]. To clearly confirm these morphological changes at the ultrastructural level, MN9D cells were treated with or without 10 nM rotenone and subjected to transmission electron microscopy. As shown in Fig. 1b, treatment of cells with rotenone for 24 h caused appearance of many swollen mitochondria within the cell. At this time point, cells still had a relatively intact membrane. However, by 36 h cells showed not only this morphological manifestation but also loss of their membrane integrity, indicating that rotenone cause quite similar morphological changes as observed in MPP^+-treated MN9D cells [14]. We then attempted to examine whether activation of caspase is involved in MN9D cells during rotenone-induced cell death. Immunofluorescent localization demonstrated that virtually no cells were positive for the cleaved form of caspase-3 in MN9D cells treated with 10 nM rotenone for 24 h or longer (Fig. 2a). This was true in MN9D cells treated with another mitochondrial complex I inhibitor, MPP^+. In contrast, treatment of cells with 100 μM 6-OHDA caused many cells positive for cleaved caspase-3 (Fig. 2a). Immunoblot analysis indicated that in MN9D cells treated with 1–100 nM rotenone, neither the cleaved caspase-9 nor the cleaved caspase-3 was detected for up to 42 h (Fig. 2b). As previously described by us [14, 17], failure to activate caspase was also observed at all concentrations of MPP^+ tested (1–100 μM, data not shown). These results were quite contrary to the robust activation of

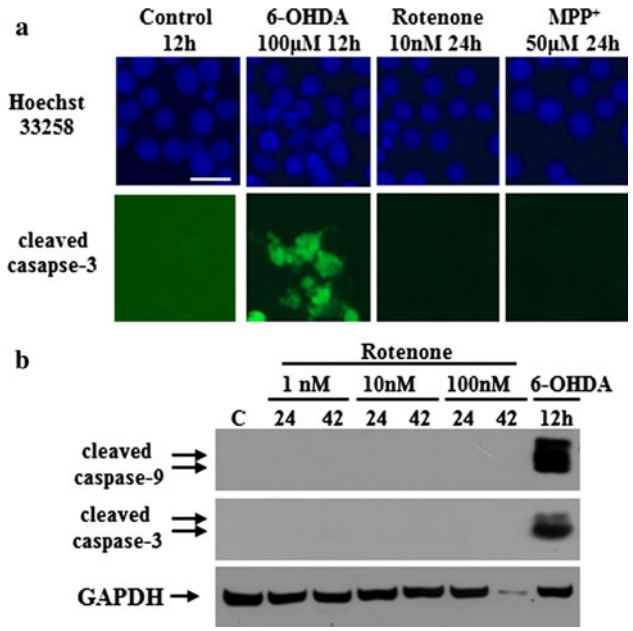

Fig. 2 Lack of caspase activation in rotenone-induced DA neurodegeneration. **a** MN9D cells treated with the indicated drugs were immunolabeled using anti-cleaved caspase-3, and then examined with a fluorescent microscopy. Nuclei were labeled with Hoechst 33258. *Scale bar* 50 μm. Photomicrographs show lack of rotenone-induced immunofluorescence for the cleaved caspase-3. **b** Cellular lysates (50 μg) were subjected to immunoblot analysis using antibodies that recognize the cleaved forms of caspase-9 and caspase-3. Lysates obtained from MN9D cells treated with 100 μM 6-OHDA were used as a positive control for caspase activation. *Blots* also show lack of caspase activation in rotenone-treated cells. Anti-GAPDH was used to confirm an equal amount of loading. All the data are the representative figure from at least three independent experiments

caspases found in 100 μM 6-OHDA-treated MN9D cells (Fig. 2b).

Cytotoxicity and caspase activity in primary cultures of DA neurons treated with rotenone

Using primary cultures of DA neurons derived from the ventral mesencephalon of E14 rat embryos, we first characterized the cytotoxic effect of rotenone on these primary cultured DA neurons by determining the rate of [^{3}H]DA uptake and the number of TH-positive neurons. From the study with concentrations ranging from 10 to 50 nM rotenone, we found a dose- and time-dependent decrease in the rate of [^{3}H]DA (Fig. 3a). Typically, a 50% reduction of DA uptake was detected at 50 nM rotenone at 48 h. After 48 h incubation with rotenone, the number of TH-positive neurons decreased in a dose-dependent manner. For example, only 30–40% of TH-positive neurons survived at 50 nM rotenone for 48 h (Fig. 3b). To determine whether caspase activation is involved in primary cultures of DA neurons following rotenone treatment, double-immunofluorescent localization of activated caspase-3 and TH was performed (Fig. 3c). Subsequently, the number of cleaved caspase-3-positive cells among TH-positive neurons was manually counted (Fig. 3d). In untreated DA neurons, virtually no TH-positive cells were shown to be positive for activated caspase-3. Following treatment with 20 μM 6-OHDA for 12 h, ~6% of TH-positive neurons were detected. In comparison with untreated DA neurons, none of the three doses of rotenone treatment induced any significant changes in the number of caspase-3-positive cells among TH-positive neurons. This was in line with our previous data demonstrating virtually no TH-positive neurons displayed immunoreactivity for the active form of caspase-3 in primary cultures of DA neurons treated with 3 μM MPP^+ [14, 17].

Depletion of cellular ATP levels in rotenone-treated cells

It was demonstrated that (d)ATP is indispensable for the formation of the apoptosome complex and subsequent activation of the caspase cascade [19]. Our previous study using MN9D cells demonstrated that MPP^+ induced a marked decrease in cellular levels of ATP while 6-OHDA did not affect the intracellular level of ATP [20]. Since rotenone is known to act on the mitochondrial electron transport chain at complex I, inducing severe defects in complex I activity and subsequent mitochondria depolarization, leading to DA neurodegeneration [6, 7, 21], we investigated whether the rotenone-induced decrease of ATP may be responsible for the lack of caspase activity. First, we determined by a luminometric measurement the absolute levels of intracellular ATP in untreated control MN9D cells. Its homeostatic levels were ranged from 8.2 to 12.6 μM as measured in four separate experiments. As shown in Fig. 4a, intracellular ATP was depleted after treatment with 10 nM rotenone in a time-dependent manner. At 24 h after rotenone, intracellular ATP decreased by up to 50% of the untreated control level, and continued to drop thereafter. We then tested whether replenishment of ATP into these cytosolic cellular lysates would restore activation of caspase-3. As shown in Fig. 4b, the addition of only 1 mM ATP to the cytosolic fraction obtained from MN9D cells treated with 10 nM rotenone for 24 h was sufficient to activate caspase-3; at a time point at which more than 50% of the intracellular ATP level was depleted. Quite similar pattern was obtained in MN9D cells treated with 50 μM MPP^+. Intriguingly, there was no sign of caspase-3 activation in the cytosolic cellular lysates harvested 36 h after drug treatment, even after the concentration of ATP was increased up to 3 mM (data not shown), indicating factor(s) other than intracellular ATP levels may be involved in the lack of caspase activation at the later phase of rotenone-induced cell death.

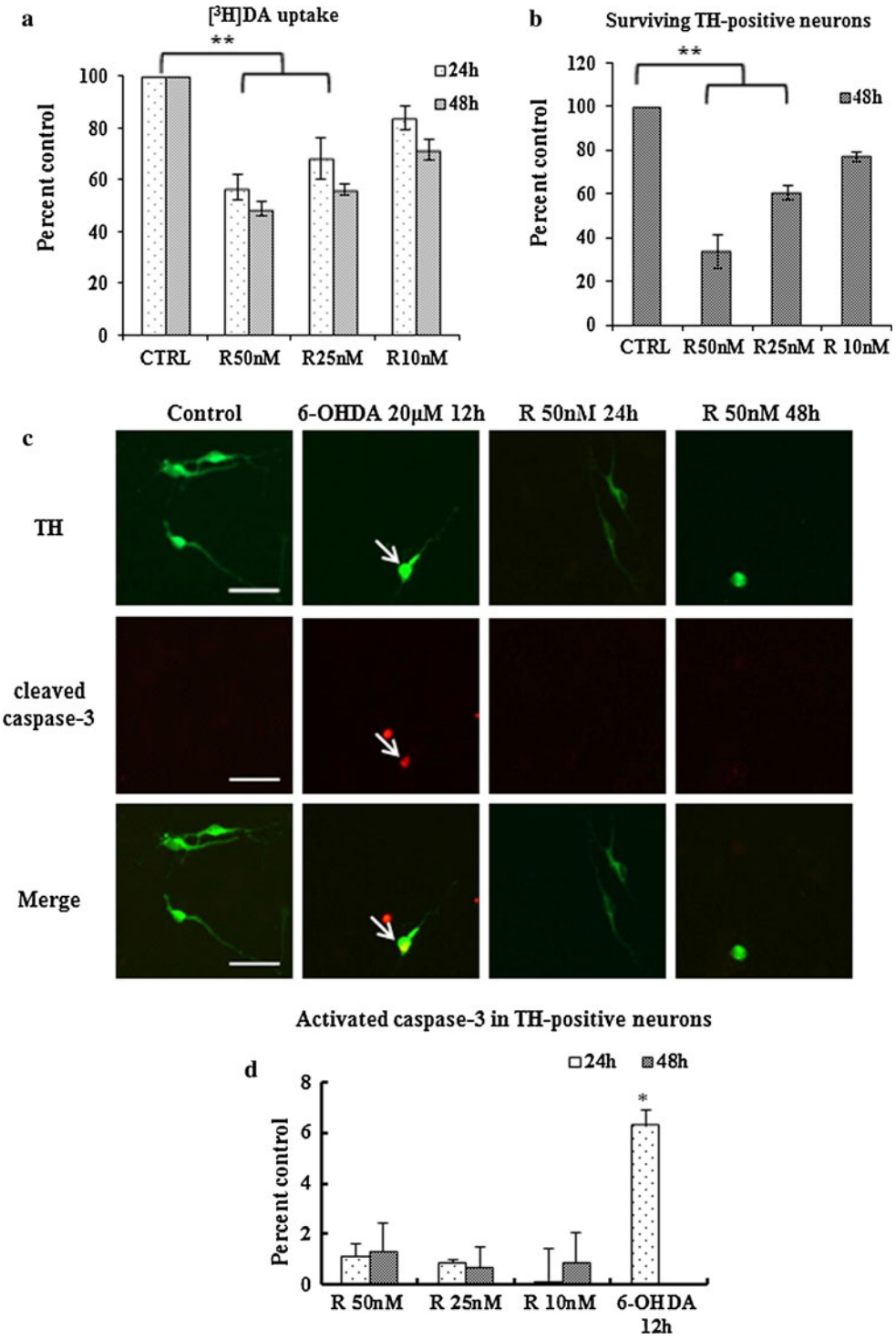

Fig. 3 Lack of caspase activity in rotenone-treated primary cultures of mesencephalic neurons. **a** Primary cultures of mesencephalic neurons treated with rotenone (R) were processed for a [^{3}H]DA uptake assay. Values from each treatment are expressed as a percentage over the untreated control (CTRL, 100%). Data represent the mean ± SEM from at least three independent experiments (**$p < 0.05$). **b** After drug treatment, cultures were immunostained for TH, and the number of surviving TH-positive neurons was counted manually. Values are expressed as a percentage over the untreated control (CTRL, 100%) and represent the mean ± SEM of three independent experiments (**$p < 0.05$). Results indicate a dose-dependent loss of DA uptake and TH-positive neurons. **c** Following drug treatment, cultures were subjected to double-immunofluorescent labeling with anti-TH (*green*) and anti-cleaved caspase-3 (*red*). *Arrow* indicates neurons that were typically positive for both activated caspase-3 and TH. *Scale bar* 50 μm. **d** Neurons that were positive for activated caspase-3 among TH-positive neurons were counted. Data represent the mean ± SEM from three independent experiments (*$p < 0.01$), indicating lack of rotenone-induced caspase activation

Degradation of procaspase-9 following rotenone treatment

The apoptosome is a large quaternary protein structure formed in response to an intrinsic or extrinsic apoptotic signal [22]. As such, Apaf-1 and cytosolically released cytochrome *c* assemble in the presence of (d)ATP to form the apoptosome complex to activate caspase cascade. We therefore attempted to examine the protein levels of other apoptosome components in rotenone-induced DA neuronal cell death to see if any of these critical components were limited at the later stage of cell death (~36 h). We found that rotenone induced a time-dependent increase in cytosolic levels of cytochrome *c* (Fig. 5a, left panel). Expression level of Apaf-1 was shown to be no different, but the level of procaspase-9 dramatically decreased at the later

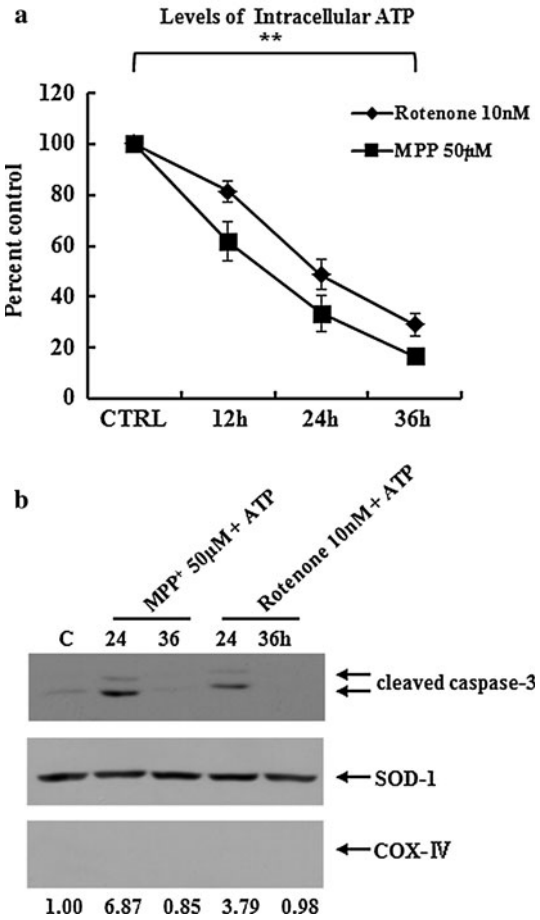

Fig. 4 Depletion of cellular ATP levels induced by rotenone treatment may be responsible for the lack of caspase activation. **a** The cellular ATP level of MN9D cells was measured before and after drug treatment and values from each treatment are expressed as a percentage relative to the untreated control (CTRL, 100%). Data from three independent cultures in triplicates are expressed as the mean ± SEM (**$p < 0.05$). **b** Following subcellular fractionation, cytosolic fractions (50 μg) were incubated in a reaction buffer with or without 1 mM ATP. Aliquots from the same reaction mixtures were subjected to immunoblot analysis for activated caspase-3. Results indicate that external addition of ATP reconstitutes the caspase-3 activity in lysates harvested 24 h after drug treatment. Cytosolic fractions were confirmed by immunoblot analysis for the presence of cytosolic marker, SOD-1 and for the absence of a mitochondrial membrane marker, COX-IV. The intensities of bands were analyzed using Image J. *Numbers below the blot* represent the average fold difference in normalized band intensity of the cleaved caspase-3 over the untreated control cells (1.00; $n = 3$)

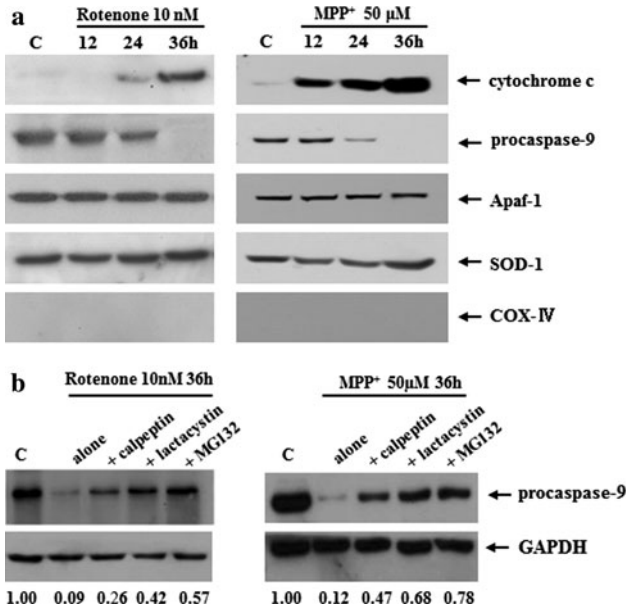

Fig. 5 Protein expression profiles of apoptosome complex following drug treatment and regulation of procaspase-9 by various protease inhibitors. **a** Following drug treatment, MN9D cells were processed to obtain the cytosolic fractions. Fractions containing the cytosolic proteins (50 μg) were analyzed by immunoblotting for cytochrome *c*, procaspase-9, or Apaf-1. *Blots* show a time-dependent increase of cytosolic cytochrome *c* and decrease of procaspase-9 levels. Duplicate blots were immunolabeled with anti-SOD-1 or anti-COX IV to confirm the cytosolic fractions of applied samples. **b** MN9D cells were treated with 10 nM rotenone or 50 μM MPP^+ in the presence or absence of various protease inhibitors. Levels of procaspase-9 from the cellular lysates were evaluated by immunoblot analysis. *Numbers below the blot* represent the average fold difference in normalized band intensity of procaspase-9 over the untreated control cells (1.00; $n = 3$). Results indicate that inhibition of calpain and proteasome activity blocks drug-induced decrease of procaspase-9

stage of cell death, and almost completely disappeared between 36 and 40 h after drug treatment. As shown in Fig. 5b (left panel), the drug-induced decrease of procaspase-9 was attenuated when MN9D cells were co-treated with 50 μM calpeptin (a calpain inhibitor), 2.5 μM MG132 (a proteasome inhibitor), or 2.5 μM lactacystin (a proteasome inhibitor), suggesting degradation of procaspase-9 may be mediated either via calpain or the proteasome. Similar patterns were observed in MPP^+-treated cells (Fig. 5a, b, right panels).

Calpain-mediated degradation of procaspase-9 in rotenone-treated cells

To investigate the possibility that rotenone indeed leads to calcium-mediated activation of calpain, we first estimated levels of intracellular free calcium in MN9D cells using Fluo-3 dye. As shown in Fig. 6a, treatment with 10 nM rotenone triggered an increase of intracellular free calcium above the control levels. With any incubation period shorter than 24 h after rotenone, no discernible levels of Fluo-3-positive cells were detected compared to that in untreated control cells (data not shown). Using an anti-fodrin antibody that only detects the ~145- or 150-kDa fragment cleaved by calpain [23], we detected the calpain-mediated cleaved fodrin in MN9D cells at all three doses of rotenone tested, and found its generation seemed to be time- and dose-dependent (Fig. 6b). Based on these data,

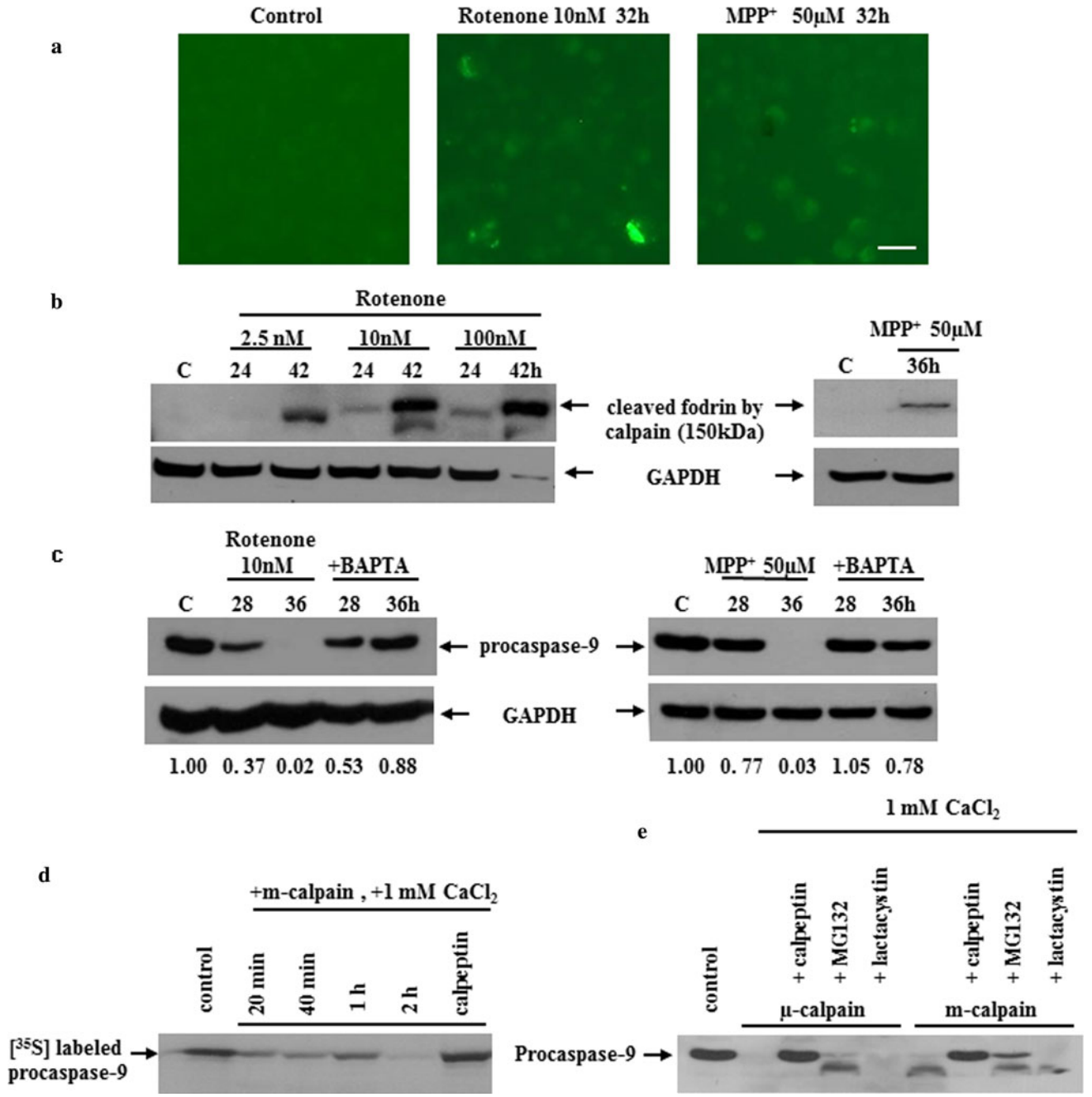

Fig. 6 Calpain-mediated degradation of procaspase-9. **a** Following drug treatment, MN9D were then stained with Fluo-3/AM dye and examined under a fluorescence microscope. *Scale bar* 50 μm. Fluorescence photomicrographs show drug-induced increase of the intracellular free calcium. **b** MN9D cells were treated with one of the varying doses of rotenone or 50 μM MPP^+ for the indicated time periods. Cellular lysates (50 μg) were subjected to immunoblot analysis using an antibody that specifically recognizes the calpain-cleaved form of fodrin [23], indicating drug-induced appearance of calpain-cleaved fodrin. **c** MN9D cells were treated with 10 nM rotenone or 50 μM MPP^+ in the presence or absence of 40 μM BAPTA/AM. Cellular lysates (50 μg) were subjected to immunoblot analysis using an antibody that specifically recognizes the procaspase-9. *Numbers below the blot* represent the average fold difference in normalized band intensity of procaspase-9 over the untreated control cells (1.00; $n = 3$), indicating that co-treatment with a calcium chelator blocks drug-induced decrease of procaspase-9. **d** [^{35}S]-labeled procaspase-9 was incubated with a reaction buffer containing 1 mM $CaCl_2$ and m-calpain in the presence or the absence of a calpain inhibitor, 5 μM calpeptin. Mixtures were separated on 10% SDS-PAGE and subjected to autoradiography. **e** Cellular lysates (50 μg) from MN9D cells were incubated with 1 mM $CaCl_2$ and μ-calpain or m-calpain in the presence or absence of various protease inhibitors. Following separation on 10% SDS-PAGE, blots were subjected to an immunoblot analysis with anti-procaspase-9 antibody, indicating a calpain-mediated cleavage of procaspase-9

we specifically asked whether the drug-induced increase in calcium levels and calpain activity was involved in the degradation of procaspase-9. As shown in Fig. 6c, drug-induced degradation of procaspase-9 in MN9D cells was largely blocked in the presence of 40 μM BAPTA-AM, an intracellular calcium chelator. The similar patterns of calcium surge and subsequent activation of calpain were also detected in MPP^+-treated samples (Fig. 6a–c; right panels). Secondly, we directly examined whether activation of calpain is responsible for the degradation of procaspase-9. In vitro transcribed and translated procaspase-9 was incubated with a purified m-calpain in the presence of 1 mM $CaCl_2$ (Fig. 6d). Autoradiogram showed a decrease in the labeled procaspase-9 that was significantly blocked in the presence of 5 μM calpeptin. To further verify this result, the cellular lysates of MN9D cells were incubated with a purified calpain in the presence of 1 mM Ca^{2+}. As shown in Fig. 6e, both μ- and m-calpain degraded procaspase-9 in the cellular lysates. Calpain-mediated degradation of procaspase-9 was largely blocked in the presence of 50 μM calpeptin but not significantly by an addition of 2.5 μM MG132 or 2.5 μM lactacystin, indicating that procaspase-9 is a substrate of the activated calpains.

Role of ubiquitin-proteasome systems in the degradation of procaspase-9 following rotenone treatment

Since MPP^+- or rotenone-induced degradation of procaspase-9 was attenuated in the presence of proteasome inhibitors (e.g., MG132 and lactacystin; see Fig. 5b), in vitro transcribed and translated full-length procaspase-9 was incubated with a reaction cocktail containing premixed E1/E2/E3 enzymes and ubiquitin-aldehyde. As shown in Fig. 7a, smeared ladder-like bands appeared, suggesting a poly-ubiquitination pattern of procaspase-9 in the reaction. To investigate whether procaspase-9 is poly-ubiquitinated during drug-induced cell death, MN9D cells transiently transfected with HA-tagged Ub plasmids were treated with 10 nM rotenone or 50 μM MPP^+ for 30 h in the presence of lactacystin. Immunoprecipitation followed by immunoblot analysis indicated that poly-ubiquitinated smear bands were detected in drug-treated sample (Fig. 7b). Considering that the intracellular levels of ATP were reduced by approximately 70% following drug treatment for 36 h, our data indicate that a few micromolar (e.g., 3 μM) ATP remained may be enough for E1 enzyme to activate ubiquitin while it is insufficient to activate caspase in drug-treated MN9D cells. Taken together, our data suggest that the ubiquitin-dependent proteasome system is also involved in degradation of procaspase-9 during rotenone-induced cell death.

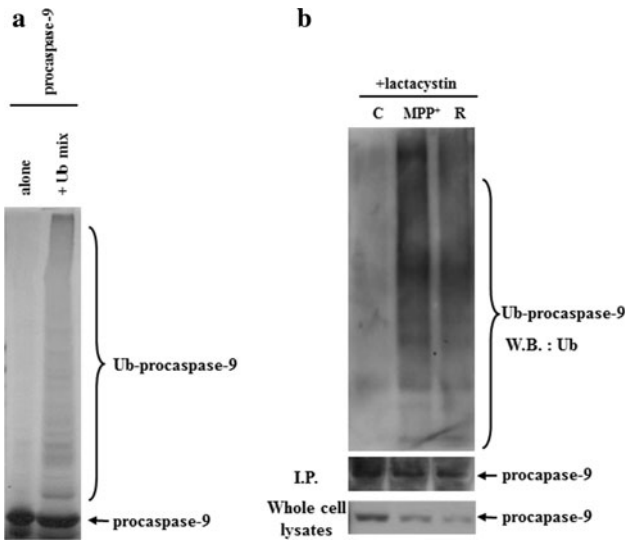

Fig. 7 In vitro and the cell-based ubiquitination assay for procaspase-9. **a** A full-length caspase-9 labeled with [^{35}S]-methionine was incubated with a reaction cocktail for ubiquitination assay. Smearing ladder-like bands with molecular weights higher than 50 kDa are shown in a lane incubated with a reaction mixture for ubiquitination assay. **b** MN9D cells transiently transfected with HA-tagged Ub plasmids were treated with or without 10 nM rotenone (R) or 50 μM MPP^+ in the presence of 2.5 μM lactacystin for 30 h. Cellular lysates were immunoprecipitated with an anti-procaspase-9 antibody and then immunoblotted with anti-ubiquitin antibodies or anti-procaspase-9 antibody, showing drug-induced appearance of smearing bands of ubiquitinated procaspase-9. Whole cell lysates were also immunoblotted with anti-procaspase-9 antibody

Reconstitution of caspase activity by co-addition of ATP and procaspase-9

To demonstrate that the lack of caspase-3 activation is due to degradation of procaspase-9 at the later phase of drug-induced cell death, we first attempted to add 1 mM ATP into the total cellular lysates harvested from rotenone-treated MN9D cells in the presence or the absence of the indicated protease inhibitors. As shown in Fig. 8a, the activated form of caspase-3 appeared to be increased when MN9D cells were treated with rotenone in the presence of either calpeptin or MG132 alone. However, simultaneous addition of both calpeptin and MG132 further increased levels of cleaved caspase-3 following drug treatment, suggesting that activation of both protease systems is responsible for the degradation of procaspase-9. To directly demonstrate this phenomenon, we performed the in vitro reconstitution assay in the presence or absence of ATP and a full length procaspase-9 using the total cell lysate obtained after rotenone treatment for 36 h. To determine the concentration of procaspase-9 present in the cytosol of MN9D cells, intracellular concentration of procaspase-9 was calculated by loading a predetermined amount of the purified procaspase-9 and comparing it with the amount in

the untreated control MN9D cells (Fig. 8b). Based on the calculated value, addition of 1 mM ATP with or without 31.25 ng procaspase-9 was selected to evaluate caspase-3 activity. As shown in Fig. 8c, simultaneous addition of ATP and procaspase-9 could reconstitute caspase-3 activity in the cellular lysates obtained following treatment with rotenone for 36 h. This indicates that simultaneous depletion of intracellular ATP and degradation of procaspase-9 are responsible for the lack of caspase activation even after cytosolic release of the mitochondrial cytochrome *c* at the later stage of drug-induced cell death.

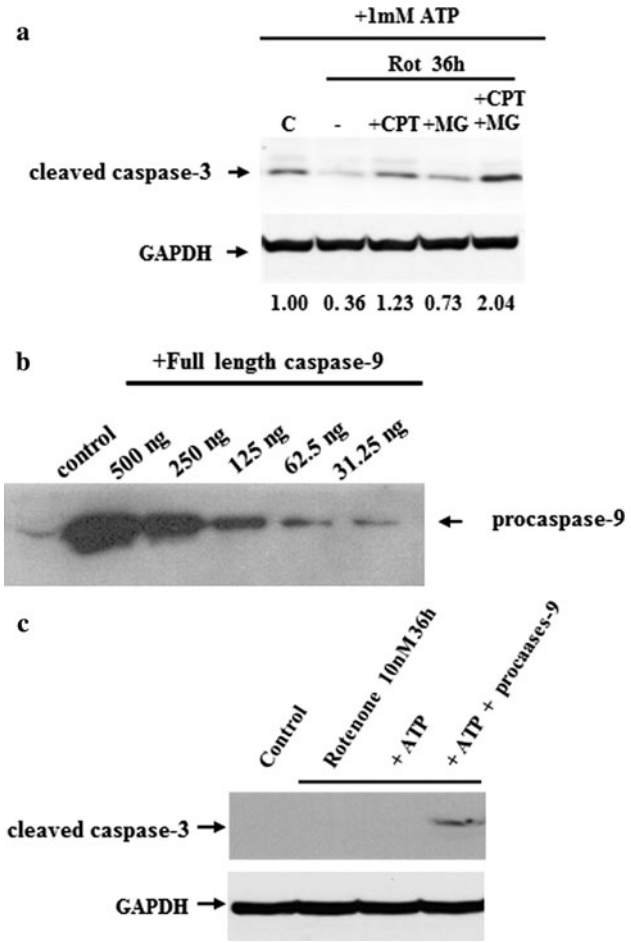

Fig. 8 Reconstitution of caspase activity following external addition of ATP and procaspase-9. **a** MN9D cells were treated with 10 nM rotenone in the presence or absence of 50 μM calpeptin (CPT), 2.5 μM MG132 (MG) or both for 36 h. Total cellular lysates (50 μg) were subjected to in vitro reconstitution of caspase activity assay with external addition of 1 mM ATP. Levels of the cleaved caspase-3 were evaluated by an immunoblot analysis. *Numbers below the blot* represent the average fold difference in normalized band intensity of the cleaved caspase-3 over the control cells (1.00; $n = 3$). **b** For quantification of endogenous level of procaspase-9 in MN9D cells, 50 μg of cellular lysates (control) and the indicated amounts of the purified full-length procaspase-9 were subjected to an immunoblot analysis with anti-procaspase-9 antibody. **c** Following drug treatment, cellular lysates (50 μg) were incubated with 1 mM ATP in the presence or absence of procaspase-9 (31.25 ng). Aliquots from the reaction mixtures were subjected to an immunoblot analysis for activated caspase-3, indicating that a simultaneous addition of ATP and procaspase-9 reconstitutes caspase activity in lysates harvested 36 h after rotenone treatment. Anti-GAPDH was used to confirm an equal amount of loading

Discussion

Previously, we have demonstrated that ROS-mediated apoptotic signaling increases after treatment with 6-OHDA and triggers activation of caspases in the MN9D DA neuronal cell line and primary cultures of cortical and mesencephalic neurons [14, 17]. Therefore, co-treatment with a caspase inhibitor significantly inhibits 6-OHDA-induced cell death in these culture models. This is largely in line with other reports using both in vitro and in vivo systems challenged with 6-OHDA. By contrast, evidence implicating the mode of cell death induced by MPP^+ is quite controversial as judged by the morphological and biochemical criteria provided in the literature. Although several previous studies provide evidence in favor of caspase-dependent apoptosis following treatment with mitochondrial complex I toxins [11–13], other reports, including some from our laboratory, have demonstrated that MPP^+-induced cell death is not typically accompanied by morphological and biochemical features of apoptosis [14–18]. Our present data demonstrate that another widely used mitochondrial complex I inhibitor, rotenone, also did not induce any apparent signs of caspase activation in both MN9D cells and primary cultures of mesencephalic neurons over a 48 h incubation period at various concentrations.

Many death-inducing stimuli often converge onto the mitochondria, causing the mitochondrial release of cytochrome *c* into the cytosol. This, in turn, leads to the formation of the apoptosome via the sequential binding of components such as Apaf-1, (d)ATP, and procaspase-9 [22]. The resulting activation of caspase-9 is typically linked to activation of the execution phase of caspases such as caspase-3, eventually leading to apoptotic cell death via cleavage of endogenous substrate proteins with critical cellular functions. In the present study, we specifically identified a case in which mitochondrial complex I inhibitor-induced release of mitochondrial cytochrome *c* into the cytosol is not linked to caspase activation in MN9D DA neuronal cells. We further provide evidence in which two critical factors are sequentially contributed to the lack of caspase activation during rotenone- or MPP^+-induced DA neurodegeneration. More specifically, we found that drug-induced depletion of intracellular ATP and the subsequent protease-mediated cleavage of procaspase-9 were responsible for the lack of caspase activation after mitochondrial

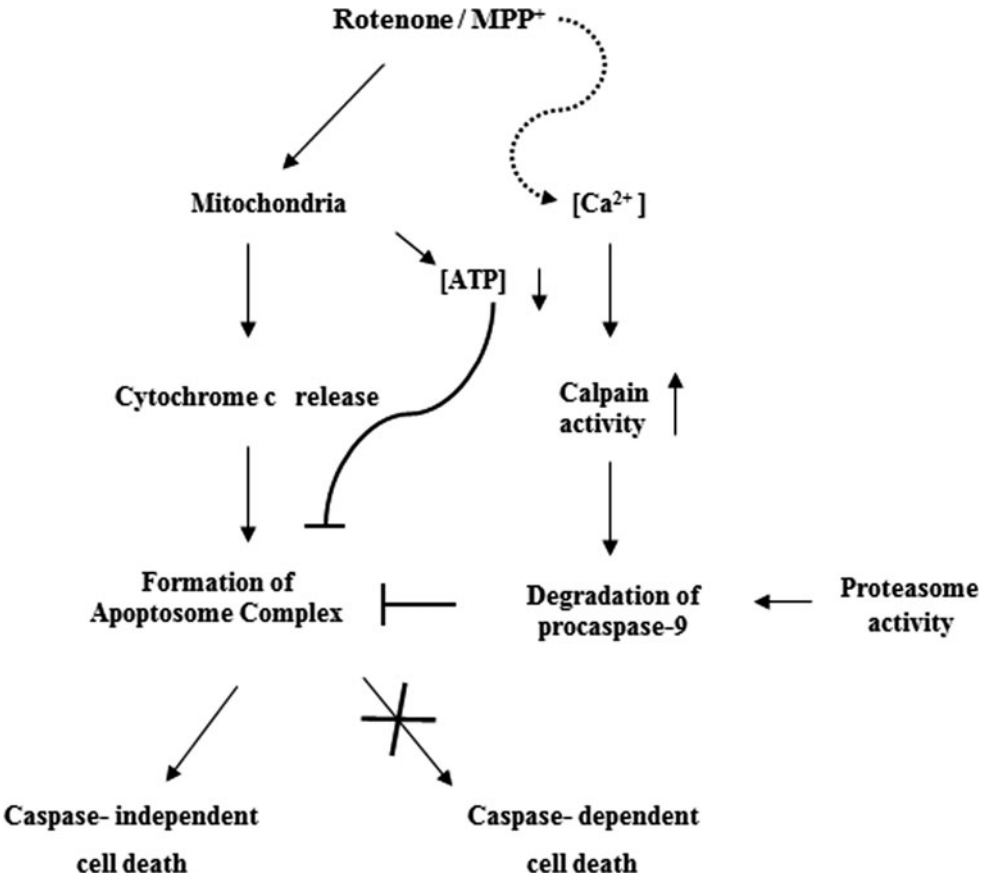

Fig. 9 Scheme of DA neuronal cell death induced by mitochondrial complex I-inhibitors. Schematic drawing demonstrates the potential mechanisms by which a time-dependent release of the mitochondrial cytochrome *c* into the cytosol is not linked to caspase activation during mitochondrial complex I inhibitor-induced DA neurodegeneration. We propose a mechanism by which both drug-induced ATP depletion and protease-mediated degradation of procaspase-9 may be responsible for preventing the formation of the apoptosome complex and contribute to the lack of caspase activation

release of cytochrome *c* (Fig. 9). Activation of both calpain and proteasome systems is critically involved in cleavage of procaspase-9. Therefore, external addition of ATP alone or in combination with procaspase-9 was necessary to reconstitute caspase activity in cellular lysates obtained at the early (<24 h) and late stage of cell death (>24 h), respectively. Therefore, our data support previous findings showing that redistribution of cytochrome *c* into the cytosol is not sufficient for, and does not always lead to, caspase activation [24–26]. We also provide an additional evidence to support the notion that modifications such as nitrosylation [27], phosphorylation [28], redox status of procaspase-9 [29], or cleavage in this study are responsible for the lack of caspase activity downstream of cytochrome *c* release. To our knowledge, our data are the first to demonstrate the mechanism by which caspase activation is checked during rotenone-induced neurodegeneration.

Calpains are a family of calcium-activated, non-lysosomal cysteine proteases [30]. Among the up to 15 identified types of calpains, there are two major isoforms, namely μ-calpain (also called calpain I) and m-calpain (calpain II), that are widely distributed in mammalian tissues. In addition to the caspases that play an important role in neuronal cell death, aberrant activation of calpains in acute and chronic neurodegeneration has also been demonstrated to lead to the cleavage of a wide variety of cellular substrates that are essential for normal physiology and neuronal survival [31]. A pathophysiological role of calcium and calcium-activated calpain in DA neurodegeneration in patients with PD has been suggested. For example, it was postulated that decreased expression levels of calbindin-D28K mRNA and protein detected in the substantia nigra may result in a failure of calcium buffering or calcium homeostasis, leading to calcium-mediated vulnerability of DA neuronal cells in this specific area of the brain [32]. Indeed, increased expression of m-calpain was localized in TH-positive nerve fibers and neuronal perikarya in the substantia nigra [33]. Crocker et al. [34] also demonstrated increased intensity in calpain-related proteolytic activity in post-mortem PD brains, as determined by immunohistochemical localization of calpain cleaved α-spectrin. Consequently, administration of a pharmacological calpain inhibitor or adenovirus-mediated overexpression of the endogenous calpain inhibitory protein, calpastatin, significantly abrogated the loss of TH-positive cells in an MPTP mouse brain model of PD [34]. As we previously demonstrated in MPP^+-induced neurodegeneration [14, 17], our present study shows that rotenone-induced cell death is also accompanied with both morphological and biochemical characteristics typical of

necrosis. These changes are indistinguishable from MPP^+-induced death. As expected, we found that co-treatment with a pan-caspase inhibitor does not block rotenone-induced cell death (data not shown). Furthermore, our preliminary data indicates that rotenone-induced neurodegeneration is significantly inhibited by the co-treatment with a cell-permeable calcium chelator or overexpression of Calbindin-D28K in MN9D cells, suggesting that calcium-mediated signaling and/or calpain activation may be critically involved in rotenone-induced neurodegeneration.

Although it remains unclear how activation of calpain contributes to DA neurodegeneration, accumulating evidence suggests that specific cleavage of the death-related proteins (e.g., Bax, p53, AIF, and α-synuclein) and transcription factors (e.g., c-Fos, c-Jun, and p35) may either directly or indirectly induce cell death (for review [31]). It is not clear whether protease-mediated cleavage of procaspase-9 itself contributes rotenone- or MPP^+-induced cell death in our study. Since any discernible fragments of procaspase-9 were not detected, and procaspase-9 seemed to be completely degraded by the combination calpain and proteasome systems, it is less likely that cleaved fragments of procaspase-9, themselves, are directly involved in drug-induced neurodegeneration in our experimental models. It has been shown that active calpain cleaves caspase-3 or -7 and this cleavage leads not only to activation but magnification of the caspase cascade in several cases, whereas cleavage of caspases by calpain leads to inactivation of caspases in other cases [35, 36]. Furthermore, a previous report by Lankiewicz et al. [37] suggested that activation of calpain converts NMDA-mediated excitotoxicity into a caspase-independent death in hippocampal culture. Similarly, inhibition of calpain activity shifts cell death from necrosis to apoptosis in 3-nitropropionic acid- and staurosporine-induced neurodegeneration [38, 39]. Along with the line of recent report indicating a central role of calpain in MPP^+-induced neurotoxicity in cerebellar granule neurons [40], our data seem to extend previous observations of cross-talk among activated proteases as typified by the result that protease-mediated degradation and inactivation of procaspase-9 blocked formation of an adequate apoptosome complex and directly contributed to caspase-independent necrotic phenomena after the mitochondrial release of cytochrome *c* in rotenone- or MPP^+-induced neurodegeneration.

Dysregulation of apoptosis, necrosis, and autophagy have been implicated in a variety of neurodegenerative disease [41]. Consequently, activation of various proteases including caspase, calpain and proteasome systems as well as lysosomal activity have all been demonstrated to be critically involved in neurodegeneration. Therefore, further studies of relative contribution and definitive regulation of these protease systems are expected to contribute to the understanding of neurodegenerative disorders and possibly lead to effective therapeutic strategies.

Acknowledgments This work was supported by a grant from the Ministry of Science and Technology through the Brain Research Center (Infra-2) and, in part, by the Mid-Career Research Program through the NRF funded by the MEST and by the KOSEF (SRC, Neurodegeneration Control Research Center at Kyung Hee University, the initial grant number R33-2008-036).

References

1. Dauer W, Przedborski S (2003) Parkinson's disease: mechanisms and models. Neuron 39(6):889–909
2. Moore DJ, West AB, Dawson VL, Dawson TM (2005) Molecular pathophysiology of Parkinson's disease. Annu Rev Neurosci 28:57–87
3. Rubinsztein DC, Gestwicki JE, Murphy LO, Klionsky DJ (2007) Potential therapeutic applications of autophagy. Nat Rev Drug Discov 6(4):304–312
4. Ungerstedt U (1968) 6-Hydroxy-dopamine induced degeneration of central monoamine neurons. Eur J Pharmacol 5(1):107–110
5. Bloem BR, Irwin I, Buruma OJ, Haan J, Roos RA, Tetrud JW, Langston JW (1990) The MPTP model: versatile contributions to the treatment of idiopathic Parkinson's disease. J Neurol Sci 97(2–3):273–293
6. Betarbet R, Sherer TB, MacKenzie G, Garcia-Osuna M, Panov AV, Greenamyre JT (2000) Chronic systemic pesticide exposure reproduces features of Parkinson's disease. Nat Neurosci 3(12):1301–1306
7. Pan-Montojo F, Anichtchik O, Dening Y, Knels L, Pursche S, Jung R, Jackson S, Gille G, Spillantini MG, Reichmann H, Funk RH (2010) Progression of Parkinson's disease pathology is reproduced by intragastric administration of rotenone in mice. PLoS ONE 5(1):e8762
8. Coulom H, Birman S (2004) Chronic exposure to rotenone models sporadic Parkinson's disease in *Drosophila melanogaster*. J Neurosci 24(48):10993–10998
9. Ryu EJ, Harding HP, Angelastro JM, Vitolo OV, Ron D, Greene LA (2002) Endoplasmic reticulum stress and the unfolded protein response in cellular models of Parkinson's disease. J Neurosci 22(24):10690–10698
10. Sherer TB, Betarbet R, Stout AK, Lund S, Baptista M, Panov AV, Cookson MR, Greenamyre JT (2002) An in vitro model of Parkinson's disease: linking mitochondrial impairment to altered alpha-synuclein metabolism and oxidative damage. J Neurosci 22(16):7006–7015
11. Viswanath V, Wu Y, Boonplueang R, Chen S, Stevenson FF, Yantiri F, Yang L, Beal MF, Andersen JK (2001) Caspase-9 activation results in downstream caspase-8 activation and bid cleavage in 1-methyl-4-phenyl-1,2,3,6-tetrahydropyridine-induced Parkinson's disease. J Neurosci 21(24):9519–9528
12. Bilsland J, Roy S, Xanthoudakis S, Nicholson DW, Han Y, Grimm E, Hefti F, Harper SJ (2002) Caspase inhibitors attenuate 1-methyl-4-phenylpyridinium toxicity in primary cultures of mesencephalic dopaminergic neurons. J Neurosci 22(7):2637–2649
13. Ahmadi FA, Linseman DA, Grammatopoulos TN, Jones SM, Bouchard RJ, Freed CR, Heidenreich KA, Zawada WM (2003) The pesticide rotenone induces caspase-3-mediated apoptosis in ventral mesencephalic dopaminergic neurons. J Neurochem 87(4):914–921
14. Choi WS, Yoon SY, Oh TH, Choi EJ, O'Malley KL, Oh YJ (1999) Two distinct mechanisms are involved in 6-hydroxydopamine- and

MPP+-induced dopaminergic neuronal cell death: role of caspases, ROS, and JNK. J Neurosci Res 57(1):86–94
15. Lotharius J, Dugan LL, O'Malley KL (1999) Distinct mechanisms underlie neurotoxin-mediated cell death in cultured dopaminergic neurons. J Neurosci 19(4):1284–1293
16. Jackson-Lewis V, Jakowec M, Burke RE, Przedborski S (1995) Time course and morphology of dopaminergic neuronal death caused by the neurotoxin 1-methyl-4-phenyl-1,2,3,6-tetrahydropyridine. Neurodegeneration 4(3):257–269
17. Han BS, Hong HS, Choi WS, Markelonis GJ, Oh TH, Oh YJ (2003) Caspase-dependent and -independent cell death pathways in primary cultures of mesencephalic dopaminergic neurons after neurotoxin treatment. J Neurosci 23(12):5069–5078
18. Li J, Spletter ML, Johnson DA, Wright LS, Svendsen CN, Johnson JA (2005) Rotenone-induced caspase 9/3-independent and -dependent cell death in undifferentiated and differentiated human neural stem cells. J Neurochem 92(3):462–476
19. Li P, Nijhawan D, Budihardjo I, Srinivasula SM, Ahmad M, Alnemri ES, Wang X (1997) Cytochrome *c* and dATP-dependent formation of Apaf-1/caspase-9 complex initiates an apoptotic protease cascade. Cell 91(4):479–489
20. Kim HE, Yoon SY, Lee JE, Choi WS, Jin BK, Oh TH, Markelonis GJ, Chun SY, Oh YJ (2001) MPP(+) downregulates mitochondrially encoded gene transcripts and their activities in dopaminergic neuronal cells: protective role of Bcl-2. Biochem Biophys Res Commun 286(3):659–665
21. Xiong N, Huang J, Zhang Z, Xiong J, Liu X, Jia M, Wang F, Chen C, Cao X, Liang Z, Sun S, Lin Z, Wang T (2009) Stereotaxical infusion of rotenone: a reliable rodent model for Parkinson's disease. PLoS ONE 4(11):e7878
22. Riedl SJ, Salvesen GS (2007) The apoptosome: signalling platform of cell death. Natl Rev Mol Cell Biol 8(5):405–413
23. Yokota M, Saido TC, Tani E, Kawashima S, Suzuki K (1995) Three distinct phases of fodrin proteolysis induced in postischemic hippocampus. Involvement of calpain and unidentified protease. Stroke 26(10):1901–1907
24. Von Ahsen O, Waterhouse NJ, Kuwana T, Newmeyer DD, Green DR (2000) The 'harmless' release of cytochrome *c*. Cell Death Differ 7(12):1192–1199
25. Borutaite V, Brown GC (2007) Mitochondrial regulation of caspase activation by cytochrome oxidase and tetramethylphenylenediamine via cytosolic cytochrome *c* redox state. J Biol Chem 282(43): 31124–31130
26. Vaughn AE, Deshmukh M (2008) Glucose metabolism inhibits apoptosis in neurons and cancer cells by redox inactivation of cytochrome *c*. Nat Cell Biol 10(12):1477–1483
27. Torok NJ, Higuchi H, Bronk S, Gores GJ (2002) Nitric oxide inhibits apoptosis downstream of cytochrome *c* release by nitrosylating caspase 9. Cancer Res 62(6):1648–1653
28. Allan LA, Morrice N, Brady S, Magee G, Pathak S, Clarke PR (2003) Inhibition of caspase-9 through phosphorylation at Thr 125 by ERK MAPK. Nat Cell Biol 5(7):647–654
29. Zech B, Kohl R, von Knethen A, Brune B (2003) Nitric oxide donors inhibit formation of the Apaf-1/caspase-9 apoptosome and activation of caspases. Biochem J 371(Pt 3):1055–1064
30. Goll DE, Thompson VF, Li H, Wei W, Cong J (2003) The calpain system. Physiol Rev 83(3):731–801
31. Vosler PS, Brennan CS, Chen J (2008) Calpain-mediated signaling mechanisms in neuronal injury and neurodegeneration. Mol Neurobiol 38(1):78–100
32. Iacopino AM, Rhoten WB, Christakos S (1990) Calcium binding protein (calbindin-D28k) gene expression in the developing and aging mouse cerebellum. Brain Res Mol Brain Res 8(4):283–290
33. Mouatt-Prigent A, Karlsson JO, Agid Y, Hirsch EC (1996) Increased M-calpain expression in the mesencephalon of patients with Parkinson's disease but not in other neurodegenerative disorders involving the mesencephalon: a role in nerve cell death? Neuroscience 73(4):979–987
34. Crocker SJ, Smith PD, Jackson-Lewis V, Lamba WR, Hayley SP, Grimm E, Callaghan SM, Slack RS, Melloni E, Przedborski S, Robertson GS, Anisman H, Merali Z, Park DS (2003) Inhibition of calpains prevents neuronal and behavioral deficits in an MPTP mouse model of Parkinson's disease. J Neurosci 23(10):4081–4091
35. Chua BT, Guo K, Li P (2000) Direct cleavage by the calcium-activated protease calpain can lead to inactivation of caspases. J Biol Chem 275(7):5131–5135
36. Sharma AK, Rohrer B (2004) Calcium-induced calpain mediates apoptosis via caspase-3 in a mouse photoreceptor cell line. J Biol Chem 279(34):35564–35572
37. Lankiewicz S, Marc Luetjens C, Truc Bui N, Krohn AJ, Poppe M, Cole GM, Saido TC, Prehn JH (2000) Activation of calpain I converts excitotoxic neuron death into a caspase-independent cell death. J Biol Chem 275(22):17064–17071
38. Pang Z, Bondada V, Sengoku T, Siman R, Geddes JW (2003) Calpain facilitates the neuron death induced by 3-nitropropionic acid and contributes to the necrotic morphology. J Neuropathol Exp Neurol 62(6):633–643
39. Neumar RW, Xu YA, Gada H, Guttmann RP, Siman R (2003) Cross-talk between calpain and caspase proteolytic systems during neuronal apoptosis. J Biol Chem 278(16):14162–14167
40. Harbison RA, Ryan KR, Wilkins HM, Schroeder EK, Loucks FA, Bouchard RJ, Linseman DA (2011) Calpain plays a central role in 1-methyl-4-phenylpyridinium (MPP(+))-induced neurotoxicity in cerebellar granule neurons. Neurotoxic Res 19(3):374–388
41. Wong E, Cuervo AM (2010) Autophagy gone awry in neurodegenerative diseases. Nat Neurosci 13(7):805–811